PHYSICAL REVIEW B **84**, 125129 (2011)

Electric-field-induced Mott transition in an organic molecular crystal

Yoshitaka Kawasugi,[1,2,3] Hiroshi M. Yamamoto,[2,3,*] Naoya Tajima,[2] Takeo Fukunaga,[2]
Kazuhito Tsukagoshi,[4] and Reizo Kato[1,2]

[1]*Saitama University, Saitama, Saitama 338-8570, Japan*
[2]*RIKEN, Hirosawa, Wako, Saitama 351-0198, Japan*
[3]*PRESTO, Japan Science and Technology Agency, Honcho Kawaguchi, Saitama 332-0012, Japan*
[4]*MANA, NIMS, Tsukuba, Ibaraki 305-0044, Japan*

(Received 31 May 2011; revised manuscript received 12 August 2011; published 16 September 2011)

We study the field effect on the strain-induced Mott-insulating state of an organic superconductor κ-(BEDT-TTF)$_2$Cu[N(CN)$_2$]Br. The gate voltage dependences of the conductivity, Hall coefficient, and thermopower were investigated. While the conductivity obeyed an activation-type insulating formula, the Hall coefficient and thermopower exhibited continuous transition to a metal-like band structure under high gate voltage. This indicates the merger of Hubbard bands at finite electrostatic doping; that is, the field-induced Mott transition.

DOI: 10.1103/PhysRevB.84.125129 PACS number(s): 73.40.Qv, 74.70.Kn, 71.27.+a

I. INTRODUCTION

Mott discussed the concept of electron correlation in a half-filled band and predicted a sharp transition from an insulating to a metallic state at a certain value of the bandwidth.[1] Hubbard extended this idea with calculations that showed that the half-filled band should be split into two so-called Hubbard bands in the insulating state.[2] The most characteristic event in the Mott transition (MT) is the merger of two (filled and empty) Hubbard bands into one half-filled band. Although Mott considered the transition under a bandwidth-controlled regime, it turned out to be possible for a change in the band filling to also evoke a decrease in the effective on-site Coulomb interaction, resulting in a similar insulator-to-metal transition.[3] The phase diagram for a Mott insulator is shown in Fig. 1(a), illustrating the concepts of bandwidth and band-filling controlled MTs as a function of U/W (U: on-site Coulomb repulsion energy; W: bandwidth) and band filling, respectively.

Chemical doping has been a typical method of modifying the Hubbard bands by band filling, and it has attracted renewed attention since high-T_c superconductivity was discovered in the doped Mott insulator, $La_{2-x}Ba_xCuO_4$.[4] Although the use of chemical doping to induce a MT is a useful method for developing new materials, the presence of the dopant always leads to the introduction of random potential fluctuations within the material. The interference between disorder and correlation becomes especially important when the system is close to the MT. The formation of a pseudogap in high-T_c cuprates is the most typical example and its relation to disorder is still not fully understood, although such an understanding is important for identifying the superconductivity mechanism.[5–8] To avoid the undesirable effects of disorder, electrostatic doping (ESD) using a field-effect transistor (FET) configuration is a useful means of investigating band-filling controlled MTs, because the degree of randomness, if any, does not change during the ESD process. Although both inorganic and organic Mott-insulator-based FET (Mott-FET) structures have already been proposed,[9–11] the simple and clear electronic structure of organic Mott insulators seems favorable for achieving experimental confirmation of a filling-controlled MT by ESD. In the meantime, the possibility of using ESD to induce a MT has also led researchers to propose a MT-FET exhibiting high performance and nanosize scalability, which makes such a device highly attractive.[11] As far as disorder without electron correlation is concerned, the concept of the "mobility edge" is useful. Anderson first pointed out that electrons cannot diffuse in their ground state when strong disorder exists in the system.[12] Mott extended this idea to the concept of the mobility edge, in which localized states exist at the bottom and top of a band and are continuously connected to extended states in the middle.[13] This concept has been very useful to understand, for example, the behavior of two-dimensional (2D) electrons in FET devices in the absence of strong electron correlation. The influence of disorder is not, however, trivial when the electron correlation is high, and this problem is frequently discussed in the Anderson-Hubbard model.[14–16] The aims of the present study include, therefore, an investigation of the influence of strong electron correlation on FET performance. We fabricated a Mott-FET with an organic Mott insulator κ-(BEDT-TTF)$_2$Cu[N(CN)$_2$]Br (κ-Br) which, in pristine form, is a superconductor at low temperature but remains in a Mott-insulating state due to a negative pressure effect when adhered as a thin crystal to a SiO_2/Si substrate [BEDT-TTF = bis(ethylenedithio)tetrathiafulvalene].[17,18] The results of transport measurements indicate that, under high gate voltage, the carriers are not located at the edge of the Hubbard band but rather at the center of the merged band. After finite ESD, the carrier density at the interface is gapless,[19] which suggests that the interfacial electrons in this device undergo a continuous transition from a Mott-insulating to a (correlation-enhanced) Anderson-insulating state. Furthermore, the carrier mobility can be tuned both by the gate voltage and thermal excitation.

κ-type BEDT-TTF salts comprise alternating layers of BEDT-TTF$^{+0.5}$ radical cations and polymeric counteranions.[20,21] Although the highest occupied molecular orbital (HOMO) band of BEDT-TTF is three-quarters filled, the dimerized structure [Fig. 1(b)] makes it effectively half-filled resulting in a Mott-insulating state. The HOMO band has a simple two-dimensional cosine dispersion and thus exhibits

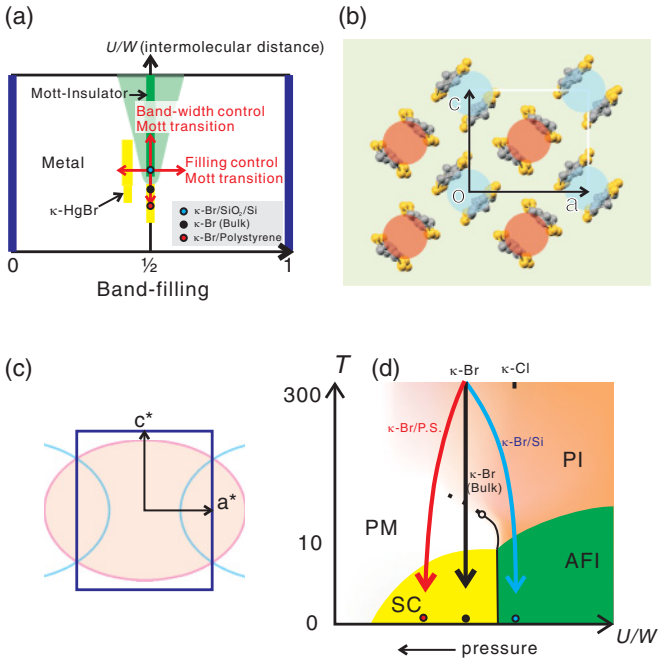

FIG. 1. (Color) (a) U/W-band filling phase diagram for the κ-BEDT-TTF system: blue, green and yellow lines denote band insulator, Mott insulator, and superconductor, respectively. The pale green area is thought to be metallic, although correlation-enhanced localization is very likely to occur. (b) Two-dimensional lattice of κ-Br viewed along the b axis. The crystallographic ac unit cell contains one red and one blue dimer in a layer (white square), each of which has one hole carrier. (c) Fermi surface of κ-Br. Since there are two dimers in the unit cell, the sectional area of the Fermi surface corresponds to 100% of the first Brillouin zone. Note that the degeneracy at the zone boundary is slightly broken resulting in anisotropic thermopower generation (Ref. 26). (d) U/W-T phase diagram for the κ-BEDT-TTF system. PI, PM, AFI, and SC denote paramagnetic insulator, paramagnetic metal, antiferromagnetic insulator, and superconductor, respectively. Blue, black, and red arrows show temperature trajectories of κ-Br for the corresponding conditions (on SiO_2/Si, bulk, and on polystyrene).

a round intersection of the Fermi surface within the a-c plane, but it is folded on the Brillouin zone boundary because of cell lattice doubling; this arrangement was first calculated by one of the authors using a tight-binding approximation [Fig. 1(c)].[22] κ-Br belongs to this class of materials and exhibits a Mott-insulator-to-metal crossover upon cooling due to bandwidth enhancement by thermal contraction,[23] followed by superconductivity whose order parameter is thought to be d-wave type [Fig. 1(d) shows the phase diagram].[20] The electronic structure of κ-Br and its family has been thoroughly investigated and its Shubnikov–de Haas oscillation,[24] Hall coefficient,[25] and thermopower measurements[26] are all, in principle, consistent with the calculated band structure, although many anomalies are known around the Mott-insulating or superconducting regions. Because the bandwidth of the family of materials κ-$(BEDT\text{-}TTF)_2Cu[N(CN)_2]Cl$ can be precisely controlled by the gas pressure, the critical behavior of the bandwidth-controlled MT in this system was comprehensively investigated by Kagawa *et al.*,[27] making κ-Br even more attractive for a study of an ESD-induced filling-controlled MT to allow a universal understanding of the MT phase diagram. At the same time, the chemically doped κ-type salt κ-$(BEDT\text{-}TTF)_4Hg_{2.89}Br_8$ (κ-HgBr) is known to show superconductivity[28] despite its large U/W. This suggests that the Mott-insulating phase of κ-type material is surrounded by a superconducting phase in the U/W-filling phase diagram, and thus field-induced superconductivity might also be possible in an organic Mott-FET based on this material.

Recently, techniques for fabricating organic FETs (OFETs) have been improving rapidly, driven by the demand for light, flexible, large-area, and printable next-generation devices. In particular, single crystal OFETs are attracting considerable attention because of their high performance and simple structure, suitable for analyzing the intrinsic nature of induced carriers in organic solids.[29–31] Using Hall coefficient measurements, the carrier density in a rubrene-based FET has been shown to coincide with the value calculated by the capacitance model,[30] and bandlike transport has been observed in the temperature and direction dependencies of the field-effect mobility.[29,31] In the present study, to fabricate a Mott-FET based on κ-Br, we have improved the lamination method used to produce single crystal OFETs by performing the lamination process in liquid alcohol to avoid breaking the fragile crystal. Here we report an electric-field-induced MT in this organic Mott-FET. Our present results indicate that the phase transition can be used as a new device tool, in which the conductivity is not driven by a change of the carrier density but is driven by a change of the carrier mobility.

II. EXPERIMENTAL

A highly doped Si substrate covered with a 200-nm-thick SiO_2 layer was cut into 3.3-mm-square dies. Crystals of κ-Br were electrochemically synthesized from a solution in which 20 mg BEDT-TTF, 100 mg $[P(C_6H_5)_4][N(CN)_2]$, and 30 mg CuBr were dissolved in 50 ml of 1,1,2-trichloroethane (10% v/v ethanol). We employed a round cell to obtain many crystals uniformly growing along a long anode. A relatively high current of 4 μA was applied for electrochemical crystallization in an Ar atmosphere. After 15 hours, several large, flat crystals (thickness: a few hundred nanometers; area: a few millimeters square) were formed along with a number of small, thick crystals. We selected one of the thin flat crystals and transferred it carefully into a container of clean alcohol (ethanol or isopropyl alcohol) using a pipette. The die-shaped substrate was also immersed in the alcohol, and the κ-Br crystal was manipulated with the tip of a strand of hair. After the crystal was placed lightly on the substrate, both were quickly removed from the liquid using tweezers. As the alcohol evaporated, the crystal became tightly adhered to the substrate. The laminated crystal can be shaped using a pulsed laser beam with a wavelength of 532 nm in order to fabricate a Hall bar or cross bar structure. The samples thus obtained have a bottom-gate FET configuration where a thin single crystal of κ-Br is used as a channel. Source and drain contacts are made using Au electrodes that have been previously evaporated on the substrate Fig. 2. We confirmed that the contact resistances are comparable to the sample resistances. The thin crystals used in this study have thicknesses of a

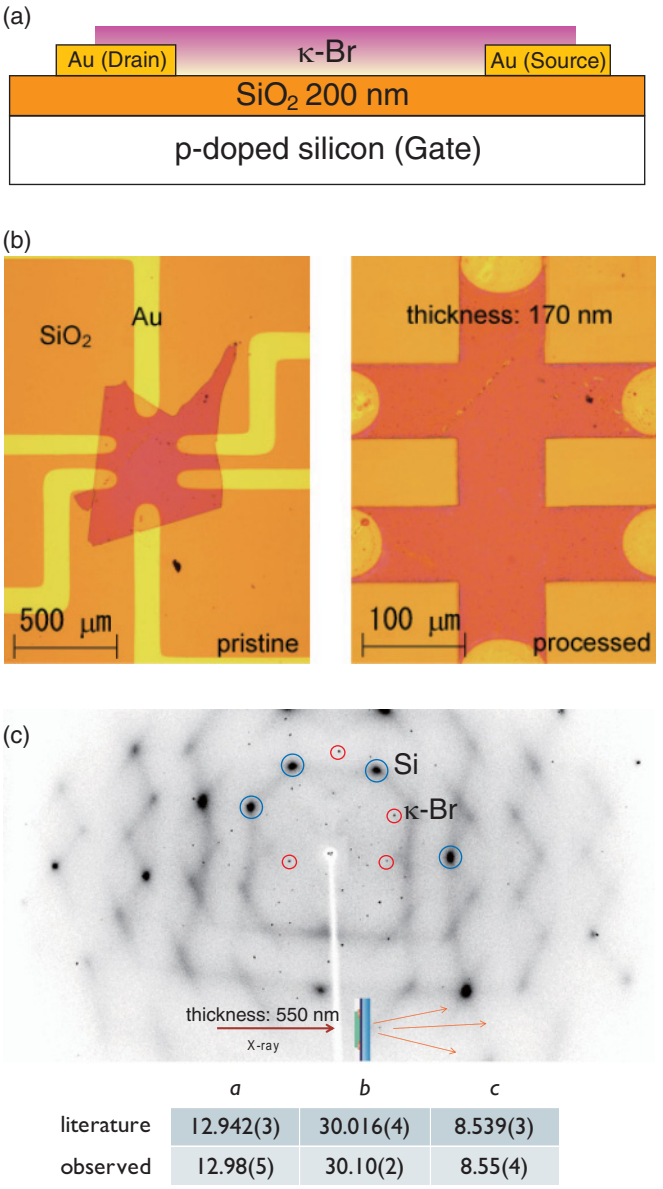

	a	b	c
literature	12.942(3)	30.016(4)	8.539(3)
observed	12.98(5)	30.10(2)	8.55(4)

FIG. 2. (Color online) (a) Schematic side view and (b) optical top view of the FET structure. (c) X-ray-diffraction pattern with incident beam normal to the substrate. The spots from a κ-Br monocrystal are observed among intense spots from Si. The bottom table shows the cell parameters from the literature (Ref. 21) and those calculated from the observations.

few hundred nanometers, and their surfaces appear flat and homogeneous based on optical microscope and step profiler measurements. Polarized microscopy observations indicate that the crystal is monocrystalline due to the presence of uniform birefringence under a crossed Nichols condition. In addition, x-ray-diffraction analysis of a laminated film (thickness: 500 nm) on a substrate showed that the film was a single crystal of κ-Br [Fig. 2(c)].

Each sample is inserted into a Physical Property Measurement System (Quantum Design, Inc.) or cryogenic chamber filled with helium. As we previously reported, the organic crystal on the substrate is subjected to strain by the substrate

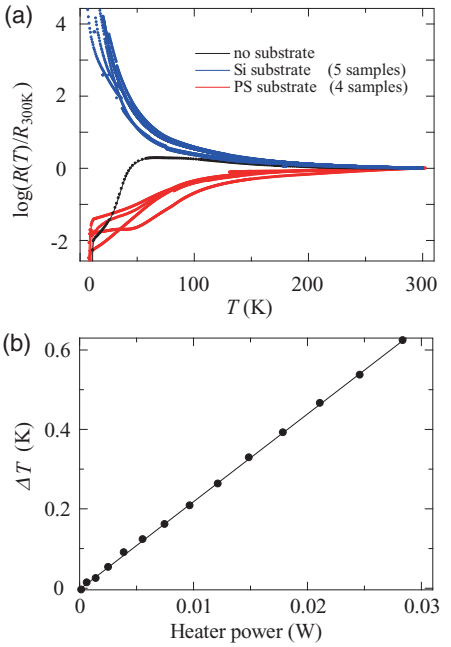

FIG. 3. (Color online) (a) Temperature dependence of the resistance of κ-Br without a substrate or adhered to silicon or polystyrene. The data for a total of ten samples are shown. (b) Temperature difference between thermometers at two opposite sample ends.

as the temperature is varied, due to mismatch of the thermal expansion coefficients.[17] This strain effect is not negligible, and it is the reason why we employed a superconducting salt, κ-Br. In the case of κ-Br, the strain effect is crucial because its ground state is located in the proximity of the Mott transition in terms of pressure. Whereas a κ-Br crystal adhered to a polymer substrate exhibited superconductivity at 10 K, the ground state of κ-Br on a Si substrate leads to the Mott-insulating phase due to the negative pressure exerted by the substrate [Fig. 3(a)]. This strain effect is reproducible across multiple samples and multiple temperature cycles with the same sample. Thus, a FET with a Mott-insulating channel can be obtained.

As well as typical Si FETs, application of gate voltage creates gradient of carrier density due to source-drain voltage. However, source-drain voltage applied in our measurements is much smaller than gate voltage (more than four orders of magnitude when $V_g \sim 100$ V). The carrier density is considered to be almost uniform along the gate insulator. On the other hand, it is difficult to determine directly the distribution of the field-induced charge along the out-of-plane direction. However, the Poisson equation applied to an OFET[32] and the dielectric constant of insulating κ-Cl (Ref. 33) suggest that the field-induced conducting layer is much thinner than one BEDT-TTF layer, implying that it is 2D under sufficient gate voltage.

For the Hall-effect measurements, the magnetic field is fixed at 8.5 T and V_g is swept, while the linearity of R_{xy} with respect to the magnetic field is checked from time to time. The simulations are carried out with the assumptions (i) the density of injected electrons is negligible compared to that of

the hole carriers and (ii) the hole density is constant. A classical formula for two different types of hole carriers is used:

$$R_H = \frac{\mu_b^2 n_b + \mu_s^2 n_s}{e(\mu_b n_b + \mu_s n_s)^2}, \quad (1)$$

where μ and n denote mobility and carrier density, and the indexes s and b stand for surface and bulk, respectively. μ_b and n_b are constant values which are measured without gate voltage. Under assumption (ii), n_s is also constant ($=1.6\times10^{14}$ cm^{-2} = 90% of the first Brillouin zone if the surface carrier is confined within one monolayer) so that the gate-voltage dependence of R_H depends on that of μ_s. Here, we employed the gate-voltage dependence of the conductivity in order to simulate how the surface mobility increases with gate voltage ($\mu_s = \sigma_s/en_s$).

The temperature gradient for the thermopower measurement is produced by heating the substrate with carbon paste resistance attached to the outer side of the sample, and the temperature of the substrate is measured by monitoring the resistance of the carbon nanotubes pasted on the substrate [Fig. 3(b)]. The temperature gradient is reversed using two heaters attached to opposite ends of the sample so as to eliminate the background.

III. RESULTS AND DISCUSSIONS

In this section we show the field effect on the electronic properties of κ-Br. See also the Supplemental Material[34] to overview the field effect on the conductivity, Hall effect, and thermopower.

A. Conductivity

Most of the samples exhibited n-type behavior with conductivity enhancement by the positive gate voltage (V_g), corresponding to electron injection. The channel conduction was almost Ohmic in the voltage range applied here and exhibited no noticeable hysteresis. The field-effect mobility is given by $\mu_{\rm FE} = (1/C_i)(d\sigma_\square/dV_g)$, where C_i is the normalized capacitance of the gate insulator and $\sigma_\square$ is the sheet conductivity. The $\mu_{\rm FE}$ values derived from the differentiated transfer curve ($d\sigma_\square/dV_g$) were quite high for OFETs, with the best sample having a value of 94 cm^2/V s, which is the highest mobility ever reported for an OFET. For single-crystal-based OFETs, the moderate enhancement of $\mu_{\rm FE}$ with cooling is often considered to be evidence for bandlike transport in devices. However, an increase of intermolecular interaction due to the thermal contraction of the crystal is another possible reason for such enhancement. On the other hand, at $V_g = 120$ V, $\mu_{\rm FE}$ clearly increases with decreasing temperature [Fig. 4(a)], despite the coefficient of thermal expansion of silicon in this temperature range being negative (i.e., the entire device must be expanded upon cooling and thus the intermolecular interaction must be decreased). This represents the first time that such an effect has been reported with cooling down to 5 K.

Figure 4 shows the logarithmic four-terminal conductivity as a function of the inverse temperature. This Arrhenius plot indicates that the transport is thermally activated and the activation energy is reduced by the application of a

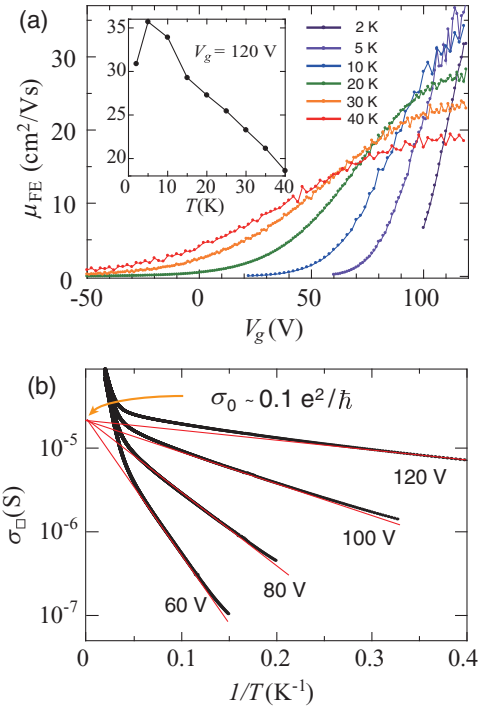

FIG. 4. (Color online) (a) Field-effect mobility estimated from $\mu_{\rm FE} = (1/C_i)(d\sigma_\square/dV_g)$. The curves of conductivity vs gate voltage were differentiated to obtain $d\sigma_\square/dV_g$. Inset shows temperature dependence of $\mu_{\rm FE}$ at $V_g = 120$ V. (b) Activation plots for the four-terminal sheet conductivity under various gate voltages. Extrapolations of the low-temperature part intersect at $1/T = 0$ with an identical prefactor σ_0.

gate voltage. While small deviation from the linearity exists possibly because of remaining electron correlation, extrapolations of the conductivity curves under gate electric fields intersect at the high temperature limit, yielding the formula $\sigma_\square = \sigma_0 \exp(-E_a/k_BT)$, where σ_0 is a constant and E_a is the gate-voltage-dependent activation energy. The fact that σ_0 is constant indicates that no macroscopic phase separation[20] occurs due to the gate voltage. In addition, the Meyer-Neldel rule,[35] by which σ_0 is dependent on the activation energy, does not apply so that transport is not governed by deep trap states. Although the above field effect is reproducible, the threshold voltage shows a sample-to-sample dependence. It tends to be negative so that most of the samples exhibited n-type behavior. However, in samples [e.g., sample no. 2: Fig. 5(b)] with a relatively high threshold voltage, ambipolar field effects have been observed as expected in Mott insulators. The shift in threshold voltage can be confirmed not only from the transfer curve but also from the dependence of the threshold voltage on the activation energy as shown in Fig. 5(c). It can be seen that the shape of the E_a vs V_g curves is similar for all samples, but $V_{\rm th}$ depends on surface conditions such as the ionic polarity of the terminal layer and the amount of impurities between the crystal and the substrate. The separation of the n-type and p-type regions implies a presence of shallow trap states between the upper and the lower Hubbard bands.

Let us now consider the activation energy E_a in the formula $\sigma_\square = \sigma_0 \exp(-E_a/k_BT)$. Since $\sigma = en\mu$, the question arises as to whether E_a originates from n, μ, or both. In typical

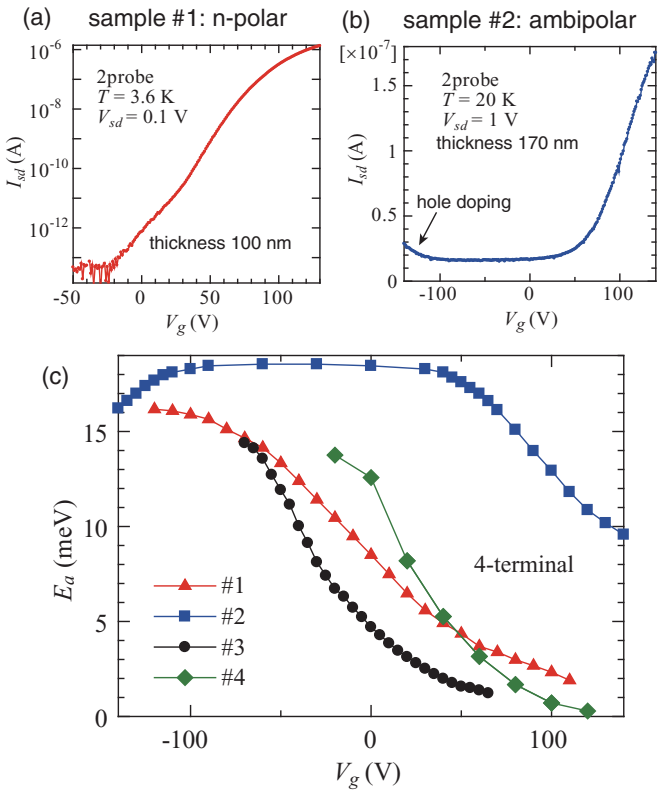

FIG. 5. (Color online) [(a),(b)] Transfer curves of n-polar (low $V_{\rm th}$) and ambipolar (high $V_{\rm th}$) samples, respectively. (c) Gate-voltage dependence of the activation energy derived from activation plots of the four-terminal conductivity. The field effect appears qualitatively similar, but the threshold voltage (horizontal position) and sensitivity to the gate voltage (slope) are sample dependent, probably due to surface conditions during fabrication.

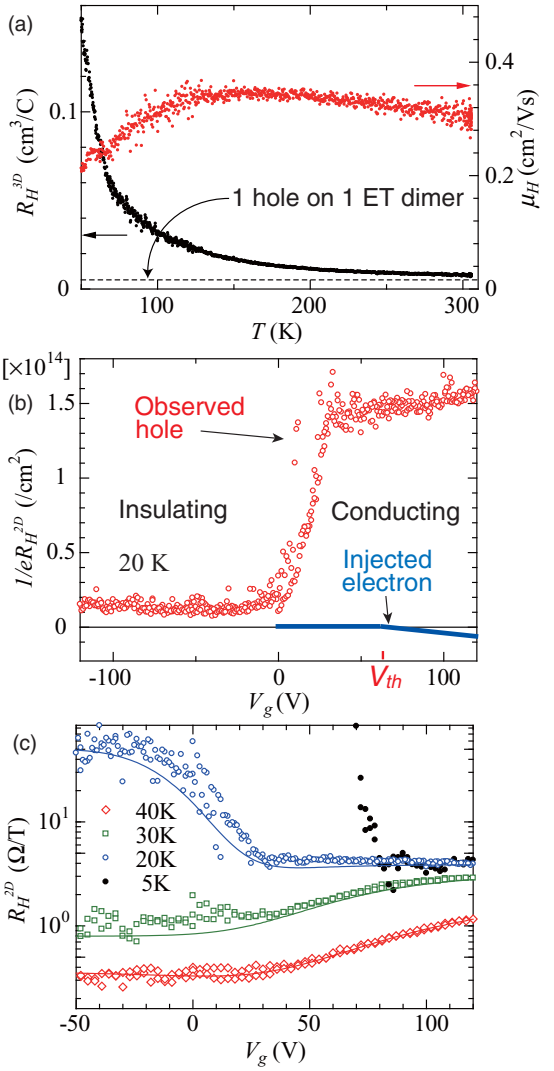

FIG. 6. (Color online) (a) Temperature dependence of the Hall coefficient and Hall mobility without gate voltage. The carrier density decreases with temperature since $n = 1/eR_H$. (b) Gate-voltage dependence of $1/eR_H$ at 20 K. The blue line denotes the density of the injected carriers calculated by the capacitance model, $Q = C(V_g - V_{\rm th})$. (c) Gate-voltage dependence of R_H at various temperatures. Solid lines show simulations at each temperature using a classical model in which field-induced and thermally activated hole carriers coexist.

semiconductors, E_a is given by the energy difference between the Fermi energy and the mobility edge which divides extended and localized states ($E_a = E_C - E_F$).[13] As the Fermi energy can be raised by the gate voltage in the rigid band of the semiconductor, E_a appears in n in a normal metal-oxide-semiconductor (MOS) FET so that only carriers beyond the mobility edge can be detected. On the other hand, the energy dispersion in a Mott insulator is not rigid against carrier doping. It is therefore necessary to check the origin of E_a, and the reason why it is reduced by gate voltage.

B. Hall effect

We next examine the carrier density using Hall-effect measurements. Figure 6(a) shows the temperature dependence of the Hall coefficient (R_H) and the Hall mobility at $V_g = 0$ V. At room temperature, we observe a Hall resistance proportional to the magnetic field, with a carrier density consistent with a model in which one dimer provides one hole carrier (1.21×10^{21} cm^{-3}). Upon cooling the sample, the carrier density is found to decrease first gradually and then sharply below 80 K, suggesting that there is an energy gap for the excitation of the carrier density. The mobility estimated from R_H and σ is, on the other hand, almost constant in the measurable temperature range [Fig. 6(a)]. The situation totally changes when a positive gate voltage is applied at low temperature. The hole carrier density sharply increases and almost saturates as the positive gate voltage is increased [Fig. 6(b)]. This is in contrast to the typical behavior where electron injection should be observed. The rigid band model seems invalid in this case as expected for a Mott-FET. Under a high gate voltage, R_H is almost constant below 20 K, and the carrier density is therefore gapless. Taking into account the fact that the hole density saturates in Fig. 6(b), we simulated R_H vs V_g plots using the classical two-carrier model with assumptions that (i) the density of injected electrons is negligible compared to that of the hole carriers and (ii) the hole density is constant (for details, see Experimental section). As shown in Fig. 6(c), the simulation reproduces the data well at

various temperatures, implying that the positive gate voltage causes an increase not in the hole density but in the hole mobility. Assuming that the active layer of the present FET is a monolayer of BEDT-TTF, as is the case with other OFETs,[36,37] the Hall coefficient under a gate voltage gives a 2D carrier density corresponding to one hole per dimer, or approximately 90% of the first Brillouin zone (1.6×10^{14} cm^{-2}). The above result suggests that the field-induced state has a high density of states comparable to the metallic (merged band) state around the Fermi level. Note that the injected electron density is only 6.7×10^{12} cm^{-2} even at $V_g = 120$ V ($V_{\rm th} = 62$ V).

C. Thermopower

The band structure of κ-Br is anisotropic because the Fermi surface protrudes over the first Brillouin zone boundary [Fig. 1(c)]. In fact, anisotropic thermopower has been reported in a bulk crystal of κ-Br, with positive (negative) values along the $a(c)$ axis.[25] If a high gate voltage recovers this anisotropy with a T-linear temperature dependence, restoration of the Fermi surface in the merged band is suggested, which coincides with the results of the Hall-effect measurements. Furthermore, a study of thermopower is likely to provide additional insights into the ground state under a gate voltage, because thermopower is thought to be almost unaffected by disorder. To measure the thermopower, a thin crystal of κ-Br was formed into a cross shape, as shown in Fig. 7(a), with the arms parallel to the a and c axes, as confirmed by polarized microscopy (cross Nichols). The arrangement of the crystal, heaters, and thermometers is shown in the figure. At room temperature, the thermopower along the a axis is clearly positive, while weak and ambiguous signals are observed along the c axis, which is the same as for measurements on bulk crystals. In the strain-induced semiconducting region, the thermopower is positive in both directions and has almost the same absolute value. The upper two panels of Fig. 7(b) show the positive thermopower dependence on the thermal gradient at $V_g = 0$ V. It exhibits semiconducting behavior, being proportional to the inverse of temperature. At temperatures below 20 K and in the absence of a gate voltage, the thermopower becomes immeasurable with the nanovoltmeter used because of the high resistance. However, it becomes measurable again when a positive high gate voltage is applied, and exhibits anisotropy along the two crystal axes [Fig. 7(b), lower two panels]. Figures 7(c) and 7(d) show the gate-voltage dependence of the Seebeck coefficient in the a and c directions, respectively. Although some data are missing because of the difficulty in the measurements, the Seebeck coefficient in the c-axis direction switches from positive to negative upon applying a high gate voltage. As shown in Fig. 7(e), at high gate voltages, the absolute value of the thermopower decreases with temperature. This suggests the presence of a T-linear component in the Seebeck coefficient, which also indicates a metalliclike behavior on the surface. We thus observed anisotropic and metallic behavior of the thermopower, whereas the conductivity remained slightly semiconducting. What is the reason for this apparent difference in the behavior of the conductivity and the thermopower? As the conductivity and Hall measurements indicate, under an applied gate voltage,

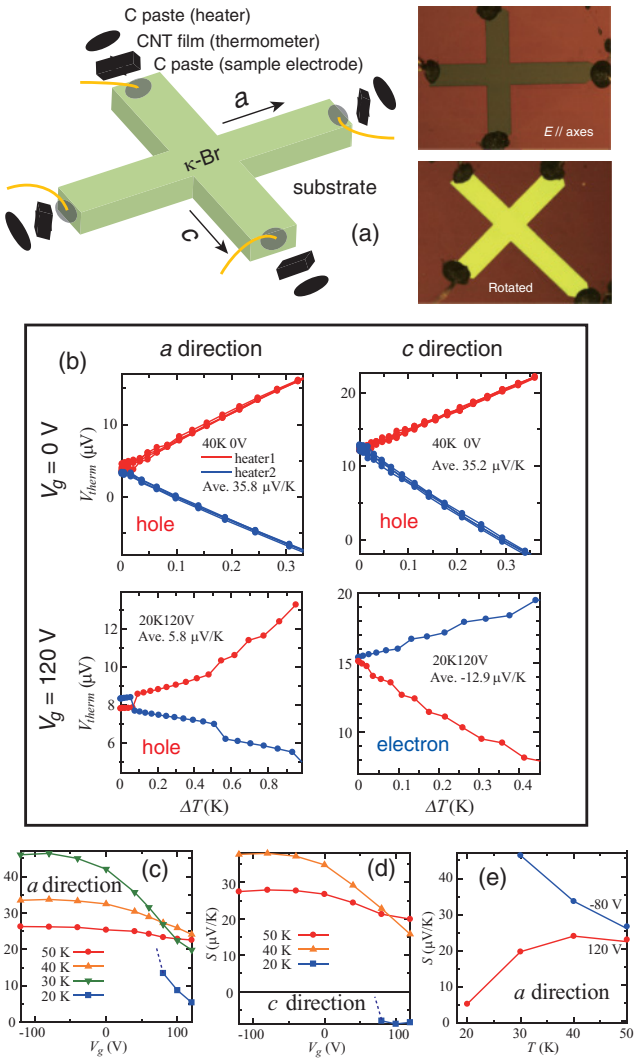

FIG. 7. (Color) (a) Schematic and optical images of the sample under the crossed Nichols condition. The heaters and thermometers are each connected with two Au wires, although the wires are omitted for clarity. (b) Temperature difference vs voltage plots at $T = 20$ and 40 K, for $V_g = 0$ and 120 V, along each crystallographic axis. The red curves show the thermopower for positive heater current (heater 1), while the blue curves show the case for heat reversal (heater 2). (c) Gate-voltage dependence of the thermopower along the a axis. (d) Gate-voltage dependence of the thermopower along the c axis. (e) Temperature dependence of the thermopower for $V_g = -80$ and 120 V, along the a axis.

the mobility of the carriers is thermally activated but the carrier density is almost temperature independent. According to Cutler and Mott,[38] the presence of disorder does not change the theory of thermopower generation because "metallic" thermopower can be observed even in hopping transport as long as there is finite density of states at the Fermi level [Eq. (9) in Ref. 35]. Actually, the thermopower in degenerate semiconductors exhibits a metallic T-linear behavior even if the conductivity remains semiconducting. Likewise, under an applied gate voltage, κ-Br can be considered to be degenerate; that is, the Fermi energy is located within an energy band, but its resistivity increases with decreasing temperature due to the microscopic hopping energy[39] that probably originates

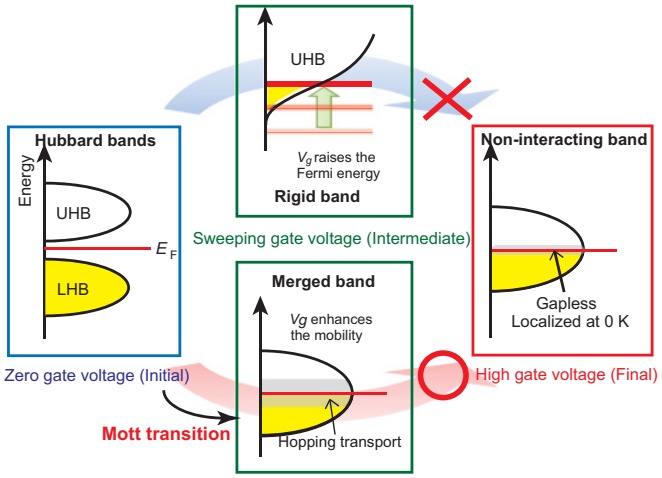

FIG. 8. (Color online) Schematics of the field effect in the Mott-insulating state of κ-Br. In the lower route, ESD enhances the screening effect and the effective Coulomb repulsive energy is reduced, resulting in a decrease in the hopping energy. The shape and amplitude of the DOS are simplified. The thickness of the shaded area in the middle of the band represents the viscosity of the carriers.

from coexisting random potential fluctuations (disorder and/or electron-lattice coupling) and Coulomb interactions.

D. Discussions

Here we discuss the effect of ESD, first considering the undoped (zero gate voltage) and highly doped (high gate voltage) states, and then examine how those states can be connected with a sweeping gate voltage. First, when no gate voltage is applied, there is an energy gap of approximately 200 K for carrier excitation, as the temperature dependence of the Hall effect shows. This effective charge gap originates from the competition between the Mott-Hubbard gap and the kinetic energy of the carriers. As long as they are observed in the Hall effect, the upper and lower Hubbard bands should be separately described in the energy spectrum of the density of states above and below the Fermi level, as shown in the left panel of Fig. 8. On the other hand, under high gate voltage, the Hall effect and conductivity results indicate a gapless state where the carrier density is temperature independent and the mobility is thermally activated, i.e., hopping transport.[38] In addition, the thermopower, which is affected very little by the random potential as discussed by Cutler and Mott, exhibits a metallic, anisotropic behavior. Since the anisotropic thermopower originates from the folding of the Fermi surface on the Brillouin zone boundary, this result suggests that the Fermi surface on the FET channels is not a small pocket but is large enough to protrude over the first Brillouin zone boundary. Therefore, it is suggested that the Fermi energy lies not in localized "tail" states, but in the middle of a band. At the same time, the carrier density derived from the Hall measurements is comparable to that in the metallic state, and the carriers are clearly holes, showing that the Fermi level is far beyond the bottom of a band. The energy spectrum is therefore formed as shown in the right panel in Fig. 8, where the upper and lower Hubbard bands have become merged, and consequently the Fermi level is located in the middle of the merged band, describing a half-filled metal. The conductivity is still semiconducting because of the thermal activation of the mobility, probably due to the effect of randomness coupled with correlation. Although it is possible that a small gap such as a soft Coulomb gap still exists, this is difficult to detect in our experiment since the system is degenerate down to 2 K. Another indication of the presence of the merged band can also be found in the monotonic decrease of $\sigma(T)$ under positive gate voltage. Since the activation energy E_a for σ can be a rough measure of the value of $E_C - E_F$ in the rigid band model, an upturn in $d\sigma/dT$ can be expected at temperatures higher than those corresponding to the observed E_a values if the Fermi level is located close to the band tail.[38] No positive $d\sigma/dT$ was observed, however, in the present study, although E_a ranges from 0.3 to 15 meV, which corresponds to 3.5–175 K. This again supports our assumption that the Fermi level is far from the bottom of the band under high gate voltage, and the conductivity is governed by thermal activation of the carrier mobility, and not by the carrier density.

Finally, we consider the path from the initial (ungated) to the final (highly gated) state based on the gate-voltage dependence of various parameters. If the rigid band model applies to the intermediate state of our Mott-FET, electron carriers should be observed in the early stages of ESD with a small positive gate voltage. In our experiment, on the other hand, we found only a sharp rise in the hole density without any signals due to independent electrons, and moreover, the hole density is too high to be induced by a conventional field effect with a SiO_2 insulator. This means that the positive gate voltage shifts the chemical potential in a direction that depletes the hole population and makes the holes better screened to result in a delocalization due to the decrease of the correlation. Therefore, it is likely that the finite doping immediately merges the Hubbard bands, and the increasing gate voltage continuously enhances the mobility of the constant-density hole carriers, as if the solidified holes entered a mobile glassy state that is originating from the effect of randomness coupled with correlation. Many of our results are consistent with theoretical considerations in the sense that no indication of phase separation is observed and divergence of the charge compressibility appears as a half-filled condition is approached.[40,41] The sudden merger of the two Hubbard bands at a finite doping level has also been addressed in a recent calculation.[42]

Although further theoretical consideration is necessary, our results describe a simple picture in which carrier doping of a Mott insulator causes the solidified holes to behave as a viscous fluid whose viscosity, characterized by the activation energy of the mobility E_a, continuously decreases with increasing ESD (i.e., increasing V_g). This observation is worth comparing to the complicated situation in high-T_c cuprates. In the case of underdoped cuprates, there appears a Fermi arc which can be regarded either as a small pocket or a dense part of a large Fermi surface. However, local disorders such as Jahn-Teller distortion and dopant effects make it difficult to discuss the underlying mechanism. The simplicity of the MT in our Mott-FET, on the other hand, allows a clean filling-controlled MT, and thus may lead to an understanding of pseudogaps in cuprates from a different angle, since the dimensionality and topology of the κ-Br Fermi surface are similar to those of cuprates.

IV. CONCLUSIONS

We observed a filling-controlled MT in a FET channel. A finite carrier doping level produced by an electric field evokes a transition from a gapped Mott insulator to a gapless surface state, which describes a simple picture of an electric-field-induced MT. The transition is rather continuous, and the conductivity is controlled by the change of carrier mobility modulated by the electrostatic-doping level. This finding clearly discriminates the mechanism of Mott-FET from that of MOS-FET. The shift in the band filling (doping concentration) in this study is not large, at most 0.04 when $V_g = 120$ V. In order to reach high doping concentrations, application of other gate insulators such as electric double layers or ferroelectric materials might be effective. The presence or absence of metallic conductivity, a pseudogap, and superconductivity at higher doping concentrations, in addition to the possibility of a room-temperature MT-FET, are subjects for future investigation.

ACKNOWLEDGMENTS

We would like to acknowledge H. Taniguchi, K. Kajita, Y. Nishio, T. Minari, Y. Takahide, and T. Hanaguri for valuable discussions, K. Kubo for helpful advice on crystal preparation, K. Yanagi for providing carbon nanotubes and S. Niitaka and H. Katori for assistance with using the instrument. This work was partially supported by Grants-in-Aid for Scientific Research (Grant Nos. 16GS0219, 20681014, and 22224006) from the Ministry of Education, Culture, Sports, Science and Technology of Japan.

*yhiroshi@riken.jp

[1] N. F. Mott, Philos. Mag. **6**, 287 (1961).
[2] J. Hubbard, Proc. R. Soc. London, Ser. A **227**, 237 (1964).
[3] M. Imada, A. Fujimori, and Y. Tokura, Rev. Mod. Phys. **70**, 1039 (1998).
[4] J. G. Bednorz and K. A. Muller, Z. Phys. B **64**, 189 (1986).
[5] A. Damascelli, Z. Hussain, and Z. Shen, Rev. Mod. Phys. **75**, 473 (2003).
[6] Y. Kohsaka, C. Taylor, P. Wahl, A. Schmidt, Jhinhwan Lee, K. Fujita, J. W. Alldredge, K. McElroy, J. Lee, H. Eisaki, S. Uchida, D. H. Lee, and J. C. Davis, Nature **454**, 1072 (2008).
[7] T. Hanaguri, Y. Kohsaka, J. C. Davis, C. Lupien, I. Yamada, M. Azuma, M. Takano, K. Ohishi, M. Ono, and H. Takagi, Nat. Phys. **3**, 865 (2007).
[8] T. Timusk and B. Statt, Rep. Prog. Phys. **62**, 61 (1999).
[9] H. Takagi and H. Y. Hwang, Science **327**, 1601 (2010).
[10] C. H. Ahn, A. Bhattacharya, M. Di Ventra, J. N. Eckstein, C. D. Frisbie, M. E. Gershenson, A. M. Goldman, I. H. Inoue, J. Mannhart, A. J. Millis, A. F. Morpurgo, D. Natelson, and J. M. Triscone, Rev. Mod. Phys. **78**, 1185 (2006).
[11] C. Zhou, D. M. Newns, J. A. Misewich, and P. C. Pattnaik, Appl. Phys. Lett. **70**, 598 (1997).
[12] P. W. Anderson, Phys. Rev. **109**, 1492 (1958).
[13] N. F. Mott, Philps. Mag. **17**, 1259 (1968).
[14] H. Shinaoka and M. Imada, Phys. Rev. Lett. **102**, 016404 (2009).
[15] M. C. O. Aguiar, V. Dobrosavljevic, E. Abrahams, and G. Kotliar, Phys. Rev. Lett. **102**, 156402 (2009).
[16] K. Byczuk, W. Hofstetter, and D. Vollhardt, Phys. Rev. Lett. **94**, 056404 (2005).
[17] Y. Kawasugi, H. M. Yamamoto, M. Hosoda, N. Tajima, T. Fukunaga, K. Tsukagoshi, and R. Kato, Appl. Phys. Lett. **92**, 243508 (2008).
[18] Y. Kawasugi, H. M. Yamamoto, N. Tajima, T. Fukunaga, K. Tsukagoshi, and R. Kato, Phys. Rev. Lett. **103**, 116801 (2009).
[19] In a mobility edge regime, the number of mobile carriers is thermally excited because the mobility remains zero in the tail state (mobility gap). On the other hand, the number of carriers in gated Mott-FET seems constant down to its ground state, even though the mobility of these carriers is continuously decreasing upon cooling. We use the term "gapless" to describe this situation where thermal excitation is not necessary to obtain a large number of mobile carriers.
[20] K. Miyagawa, K. Kanoda, and A. Kawamoto, Chem. Rev. **104**, 5635 (2004).
[21] A. M. Kini, U. Geiser, H. H. Wang, K. D. Carlson, J. M. Williams, W. K. Kwok, D. G. Vandervoort, J. E. Thompson, D. L. Stupka, D. Jung, and M.-H. Whangbo, Inorg. Chem. **29**, 2555 (1990).
[22] A. Kobayashi, R. Kato, H. Kobayashi, S. Moriyama, Y. Nishio, K. Kajita, and W. Sasaki, Chem. Lett. **1987**, 459 (1987).
[23] M. Kund, H. Muller, N. D. Kushch, K. Andres, and G. Saito, Synth. Met. **70**, 951 (1995).
[24] K. Oshima, T. Mori, H. Inokuchi, H. Urayama, H. Yamochi, and G. Saito, Phys. Rev. B **38**, 938 (1988).
[25] K. Murata, M. Ishibashi, Y. Honda, N. A. Fortune, M. Tokumoto, N. Kinoshita, and H. Anzai, Solid State Commun. **76**, 377 (1990).
[26] R. C. Yu, J. M. Williams, H. H. Wang, J. E. Thompson, A. M. Kini, K. D. Carlson, J. Ren, M.-H. Whangbo, and P. M. M. Chaikin, Phys. Rev. B **44**, 6932 (1991).
[27] F. Kagawa, K. Miyagawa, and K. Kanoda, Nature **436**, 534 (2005).
[28] H. Taniguchi, T. Okuhata, T. Nagai, K. Satoh, N. Mori, Y. Shimizu, M. Hedo, and Y. Uwatoko, J. Phys. Soc. Jpn. **76**, 113709 (2007).
[29] V. C. Sundar, J. Zaumseil, V. Podzorov, E. Menard, R. L. Willett, T. Someya, M. E. Gershenson, and J. A. Rogers, Science **303**, 1644 (2004).
[30] J. Takeya, J. Kato, K. Hara, M. Yamagishi, R. Hirahara, K. Yamada, Y. Nakazawa, S. Ikehata, K. Tsukagoshi, Y. Aoyagi, T. Takenobu, and Y. Iwasa, Phys. Rev. Lett. **98**, 196804 (2007).
[31] K. P. Pernstich, B. Rossner, and B. Batlogg, Nat. Mater. **7**, 321 (2008).
[32] G. Horowitz, M. E. Hajlaoui, and R. Hajlaoui, J. Appl. Phys. **87**, 4456 (2000).
[33] Y. Takahide, M. Kimata, K. Kodama, T. Terashima, S. Uji, M. Kobayashi, and H. M. Yamamoto, Phys. Rev. B **84**, 035129 (2011).
[34] See Supplemental Material at http://link.aps.org/supplemental/10.1103/PhysRevB.84.125129 for temperature dependence of the conductivity, Hall coefficient, and thermopower at different gate voltage.
[35] W. Meyer and H. Neldel, Z. Tech. Phys. **12**, 588 (1937).
[36] M. Kiguchi, M. Nakayama, T. Shimada, and K. Saiki, Phys. Rev. B **71**, 035332 (2005).

[37]G. Horowitz, M. E. Hajlaoui, and R. Hajlaoui, J. Appl. Phys. **87**, 4456 (2000).
[38]M. Cutler and N. F. Mott, Phys. Rev. **181**, 1336 (1969).
[39]M. H. Cohen, E. N. Economou, and C. M. Soukoulis, Phys. Rev. B **30**, 4493 (1984).
[40]N. Furukawa and M. Imada, J. Phys. Soc. Jpn. **60**, 3604 (1991).
[41]G. Kotliar, S. Murthy, and M. J. Rozenberg, Phys. Rev. Lett. **89**, 046401 (2002).
[42]S. Sakai, Y. Motome, and M. Imada, Phys. Rev. Lett. **102**, 056404 (2009).